SAND2016-2687C

Shale-brine-CO_2 interactions and the long-term stability of shale caprock

Anastasia Ilgen[1]
T. Stewart[1], J. Feldman[1], J. Major[2], P. Eichhubl[2], M. Aman[2], N. Espinoza[2], C. Choens[1], T. Dewers[1] , and P. Newell[1]

[1]Sandia National Laboratories
[2]University of Texas at Austin

U.S. DEPARTMENT OF ENERGY | Office of Science

CFSES Center for Frontiers of Subsurface Energy Security

THE UNIVERSITY OF TEXAS AT AUSTIN

Sandia National Laboratories

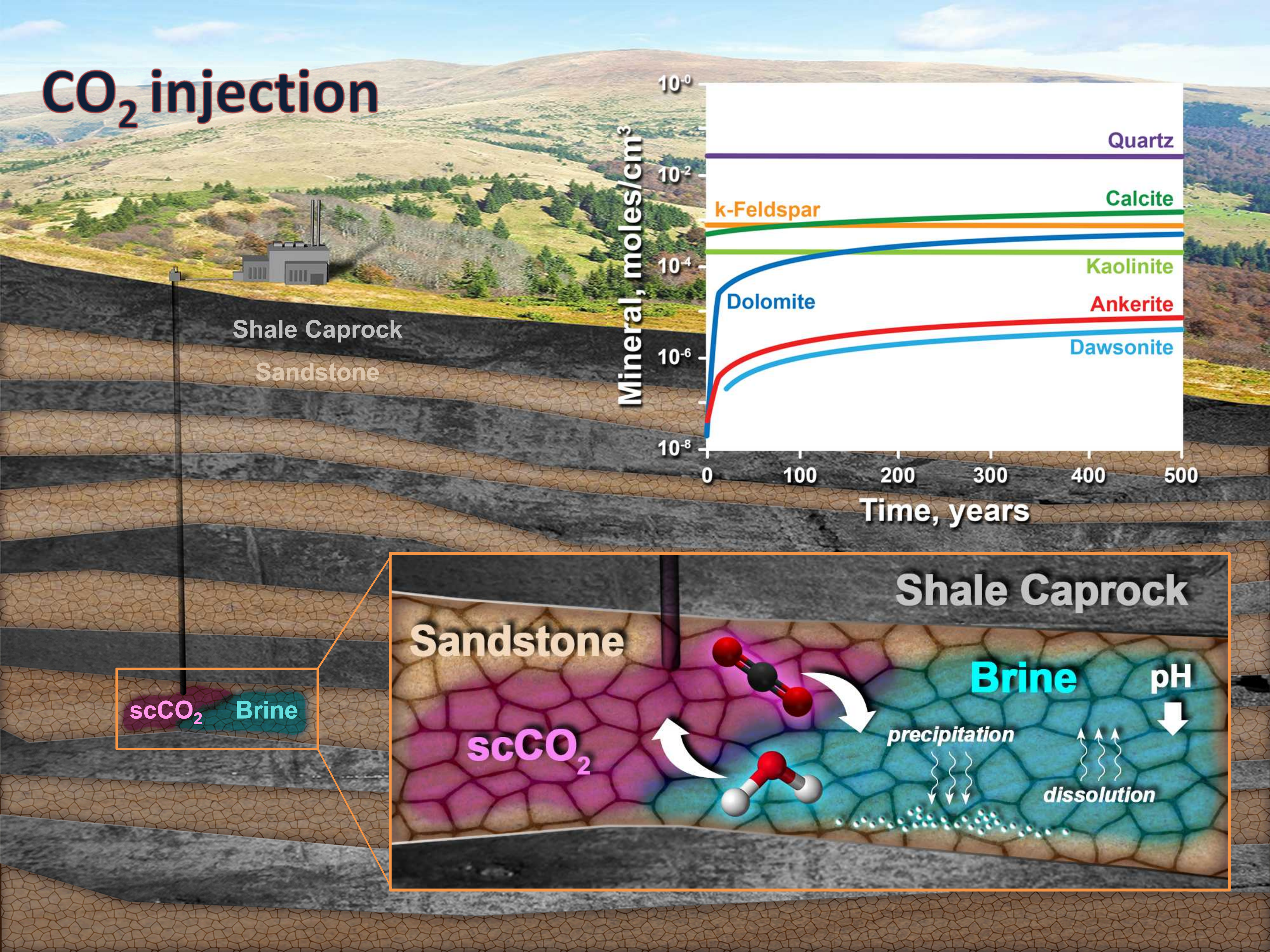

CO2 injection
Mineral, moles/cm3
10-0
10-2
10-4
10-6
10-8
Quartz
Calcite
k-Feldspar
Kaolinite
Dolomite
Ankerite
Dawsonite
0
100
200
300
400
500
Time, years
Shale Caprock
Sandstone
scCO2
Brine
Shale Caprock
Sandstone
Brine
pH
scCO2
precipitation
dissolution

Geochemical response triggered by the injection of CO_2

- At geologic storage PT: CO_2 is supercritical ($scCO_2$).
- $scCO_2$ stimulates **geochemical responses**: acidification of parent brine, and dehydration of mineral surfaces.[1-3, 8]
- Experimental and field studies: geochemical reactions differ significantly for different rock assemblages and brine compositions.[7-9]
- Low-permeability caprocks (shale) are reactive at the higher end of the geologic carbon storage temperature range.[10, 11]
- Dissolution and secondary mineral precipitation control the evolution of **porosity** and **permeability** [8], with potential impact on the caprock integrity, and CO_2 leakage.[10, 12]

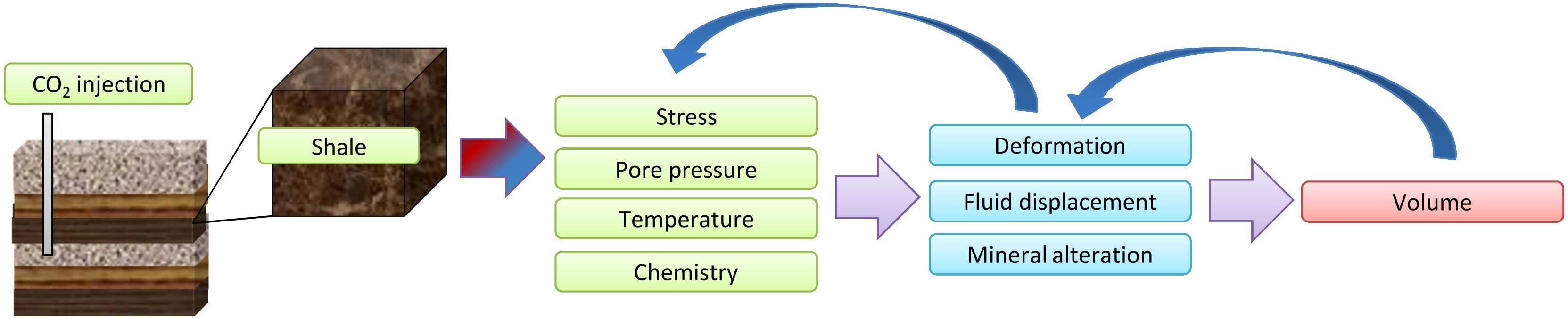

[1] DePaolo et al., 2013
[2] Marini, 2006
[3] Kharaka and Cole, 2011
[4] Kobos et al., 2011
[5] Steele-MacInnis et al., 2012
[6] Gilfillan et al., 2009
[7] Bickle et al., 2013
[8] Jun et al., 2012
[9] Lu et al., 2012
[10] Liu et al., 2012
[11] Kaszuba et al., 2003
[12] Harvey et al., 2012

Coupled chemo-mechanical processes in shale caprock

- **Objectives of this activity**
  - Establish quantitative relationships between chemical reactions triggered by the addition of supercritical CO_2 and changes in nano- to micro-scale mechanical properties of shale.
- **Team & Roles**
  - Anastasia Ilgen: shale characterization, alteration, and geochemical modeling
  - Tom Stewart: alteration experiments
  - Josh Feldman: alteration experiments
  - Jon Major: Crystal Geyser field study, geomechanical experiments
  - Peter Eichhubl: Crystal Geyser field study, geomechanical experiments
  - Michael Aman: micromechanical characterization, scratch and indentation
  - Nicolas Espinoza: micromechanical characterization, scratch and indentation
  - Charles Choens: micromechanical characterization, micro-pillar indentation
  - Tom Dewers: micromechanical characterization, micro-pillar indentation
  - Pania Newell: modeling

Coupled chemo-mechanical processes in shale caprock

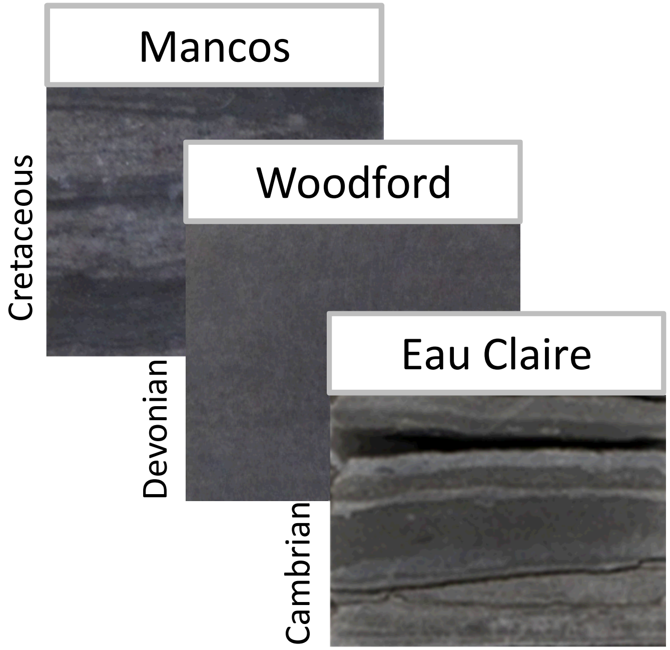

- **<u>Laboratory experiments</u>** on shale samples at conditions typical of GCS to understand time-dependent geochemical reactions.
- Geochemical modeling for data interpretation.
- Nano- and micro-mechanical characterization to understand chemical effects on mechanical properties in heterogeneous shale caprock.

- **<u>Field Study</u>** on shale and sandstone to understand fractures in natural CO_2 reservoir caprock: Crystal Geyser analog site.
- Mechanical characterization to understand chemical effects on mechanical properties in shale caprock.

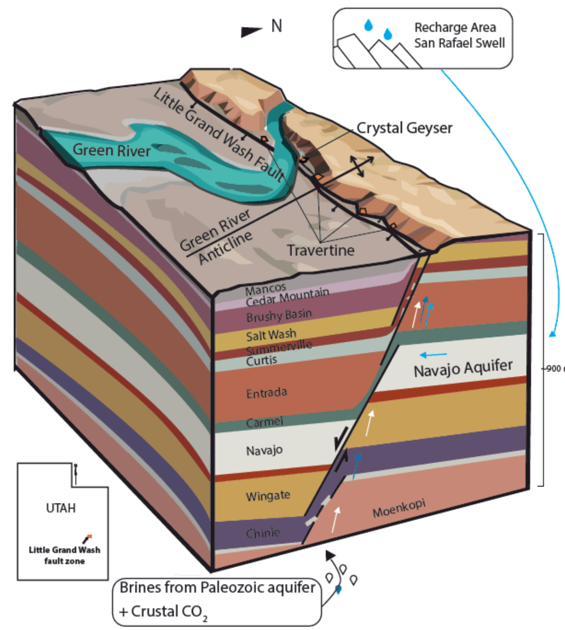

Mineral alteration

- Dissolution of **feldspars** and **phyllosilicate minerals**, dissolution and re-precipitation of **carbonate** and **clay minerals** [1].

$$\mathbf{Fe_{2.5}Mg_{2.5}Al_2Si_3O_{10}(OH)_8} + \mathbf{2.5CaCO_3} + 5CO_2 \rightarrow \quad [2]$$

chlorite calcite

$$\rightarrow 2.5FeCO_3 + 2.5MgCa(CO_3)_2 + Al_2Si_2O_5(OH)_4 + SiO_2 + 2H_2O$$

siderite dolomite kaolinite chalcedony

$$\mathbf{KMg_{2.87}Si_{3.07}Al_{1.23}O_{10}(OH)_2} + H_2CO_3 + Na^+ + Cl^- \rightarrow \quad [3]$$

phlogopite

$$\rightarrow (K,H_3O)(Al,Mg)_2(Si,Al)_4O_{10}[(OH)_2,(H_2O)] + SiO_{2(am)} + AlOOH_{(s)} +$$

illite diaspore

$$+ NaCl + K^+ + Mg^{2+} + Al^{3+} + H_4SiO_4 + HCO_3$$

$$\mathbf{2NaAlSi_3O_{8(s)}} + H^+ + 0.5H_2O \rightarrow AlO(OH)_{(s)} + 0.5Al_2Si_2O_5(OH)_{4(s)} + 2Na^+ + 5SiO_2 \quad [4]$$

albite boehmite kaolinite

$$\mathbf{CaCO_{3(s)}} + 2H^+ \rightarrow Ca^{2+} + H_2CO_3$$

calcite

[1] Liu et al., 2012
[2] Gaus et al., 2010
[3] Garcia et al., 2012
[4] Fu et al., 2009

Shale alteration in brine-CO_2 mixtures

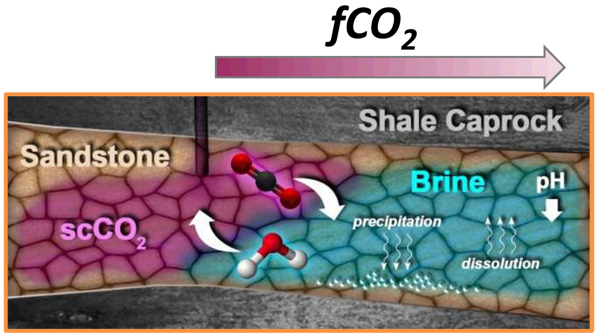

- Stirred reactors pressurized with **CO_2**
- Control reactors – **N_2** or ambient atm
- Powdered shale (A_{BET} = 8.3 m^2 g^{-1}) + **brine**
- Sample brine and solids at time intervals
- Analysis by IC, ICP-MS, and XRD
- Geochemical modeling

Shale alteration in brine-CO_2 mixtures

Mancos

Synthetic brine*

pH	7.44	I = 1.45 M
Cl^-	1589	mg/L
NO_3^-	4.1	mg/L
SO_4^{2-}	47251	mg/L
K^+	20.5	mg/L
Ca^{2+}	484	mg/L
Na^+	19000	mg/L
Mg^{2+}	2700	mg/L
Fe^{2+}	2	mg/L

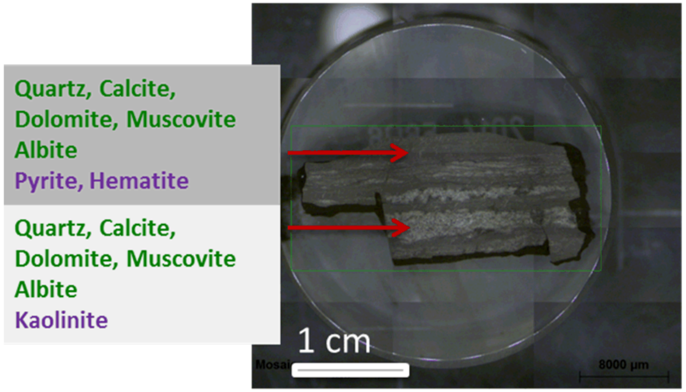

Estimated solubility of CO_2 in brine = 0.84 M**

* Developed based on the dataset from "Natural Contamination from the Mancos Shale" Report, US DOE, ESL–RPT–2011–01.
** Using Duan and Sun (2003) data for NaCl.

Woodford

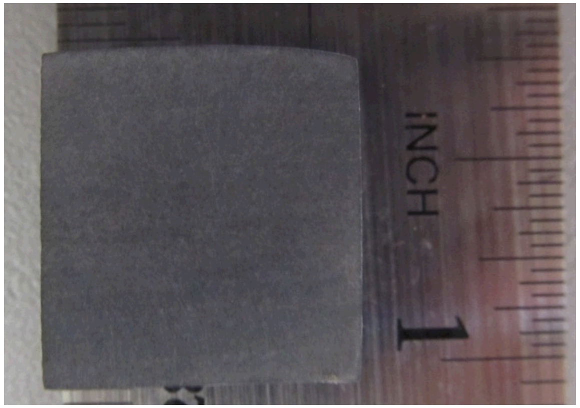

Synthetic brine**

pH	6.5	I = 0.26 M
Cl^-	8651	mg/L
HCO_3^-	1100	mg/L
SO_4^{2-}	82	mg/L
Ca^{2+}	65	mg/L
Na^+	5910	mg/L
Mg^{2+}	20	mg/L

* *Developed based on U.S. Geological Survey National Produced Waters Geochemical Database v2.1, Woodford shale

Aqueous chemistry: Mancos

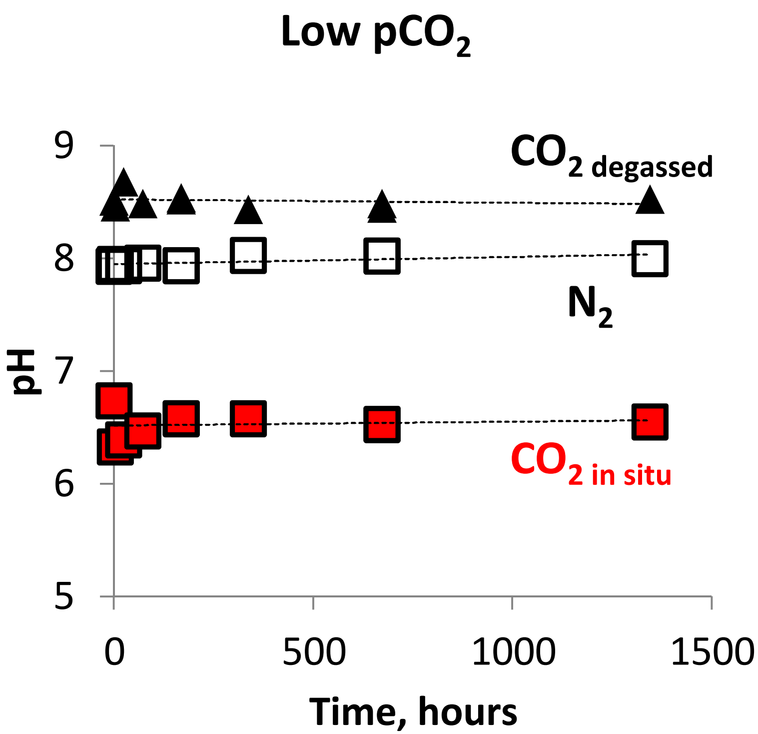

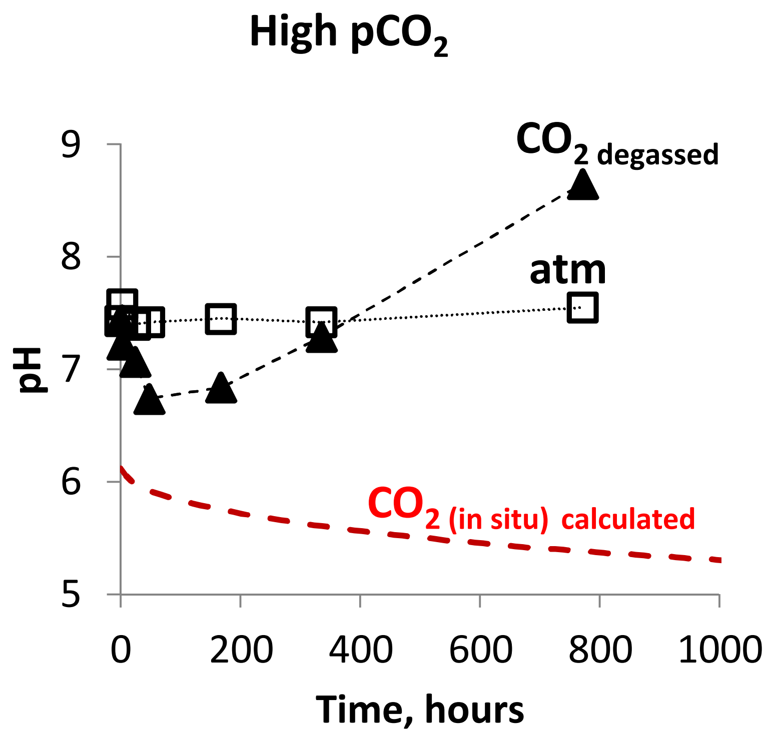

- pH is buffered by the dissolution of CO_2 into brine, and dissolution of carbonates.

Aqueous chemistry: Mancos

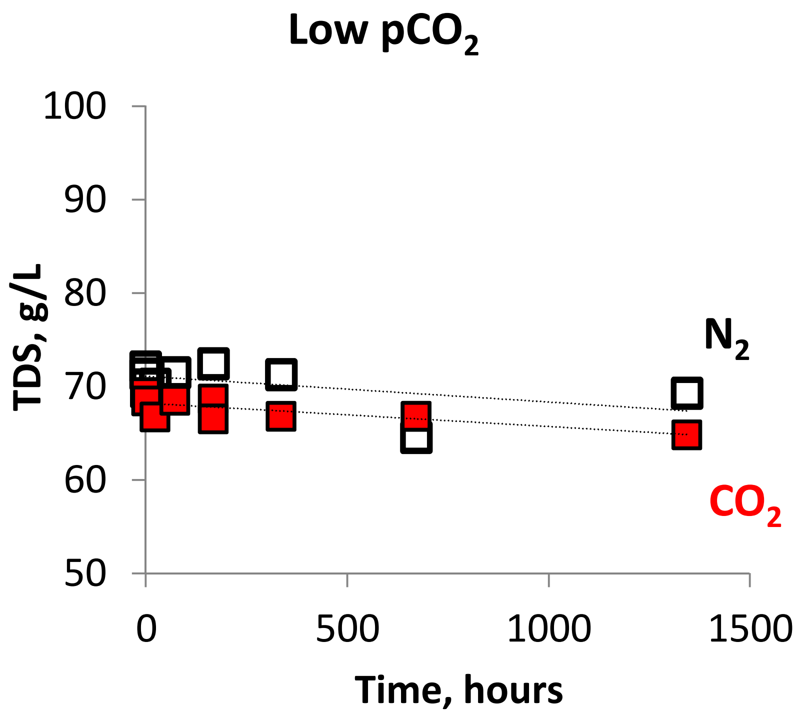

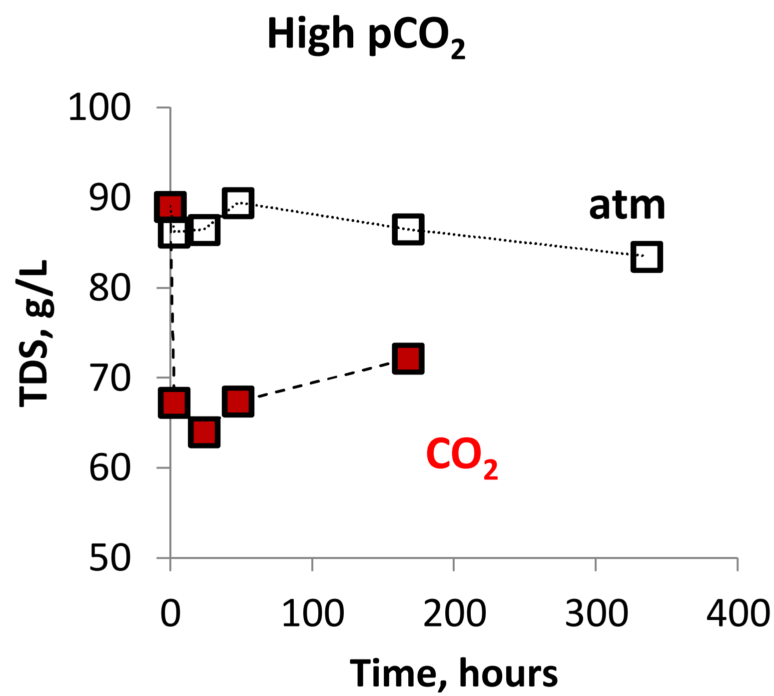

- Decrease in TDS in low and high pCO_2 reactors, and control reactors.
- Positive Na-K correlation indicates no cation exchange.
- Ca and Sr are more soluble in high pCO_2 vs. control reactors.
- Very low (microM) Fe - Fe is more soluble in high p-CO_2 -pressurized reactor.
- Al – below the detection limit.

Geochemical modeling: Mancos

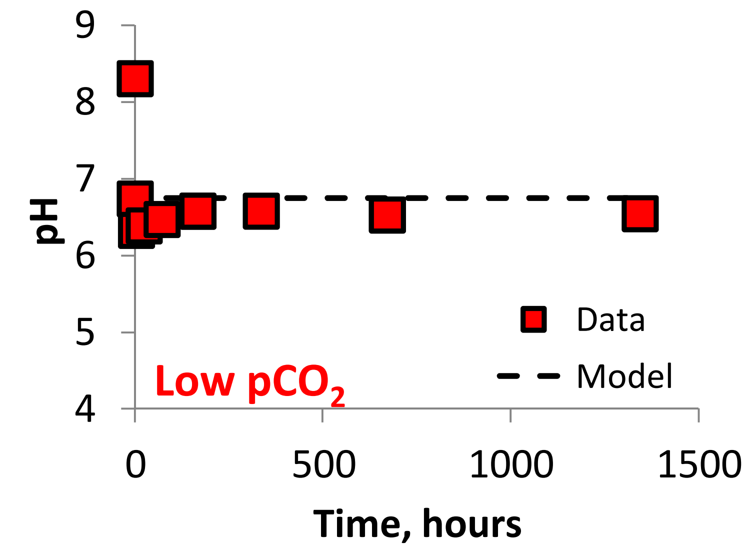

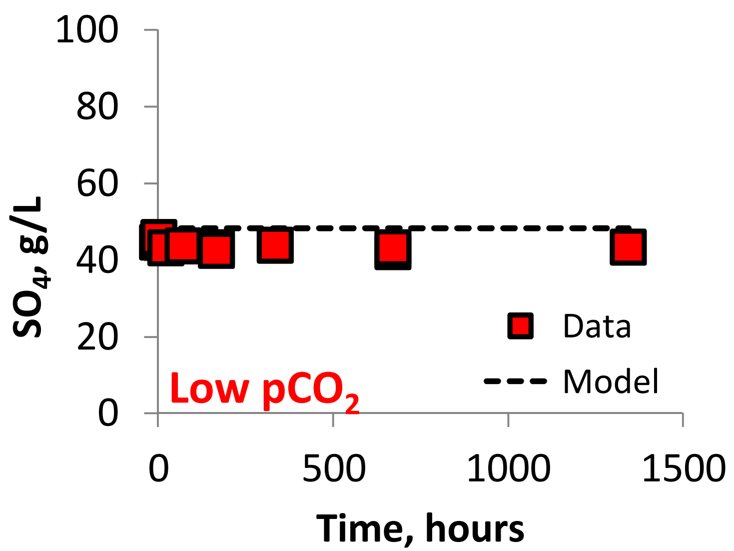

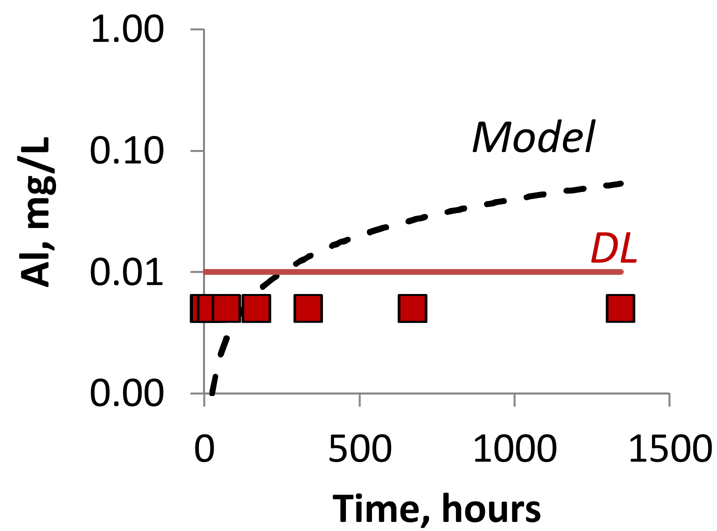

- Geochemical models capture major trends, but not everything (yet!).

Geochemical modeling: Mancos

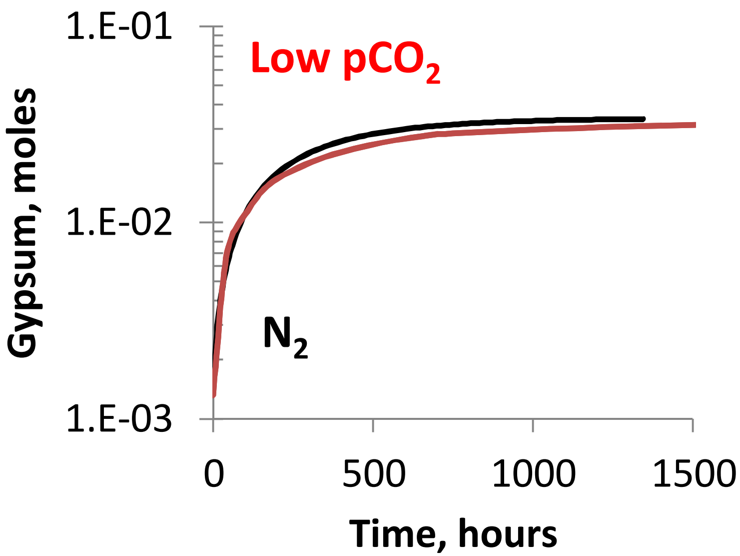

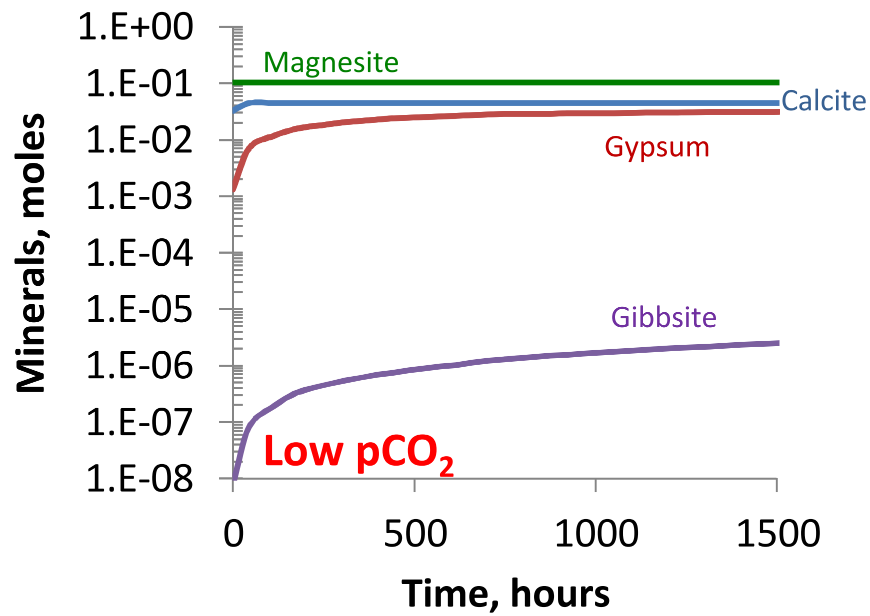

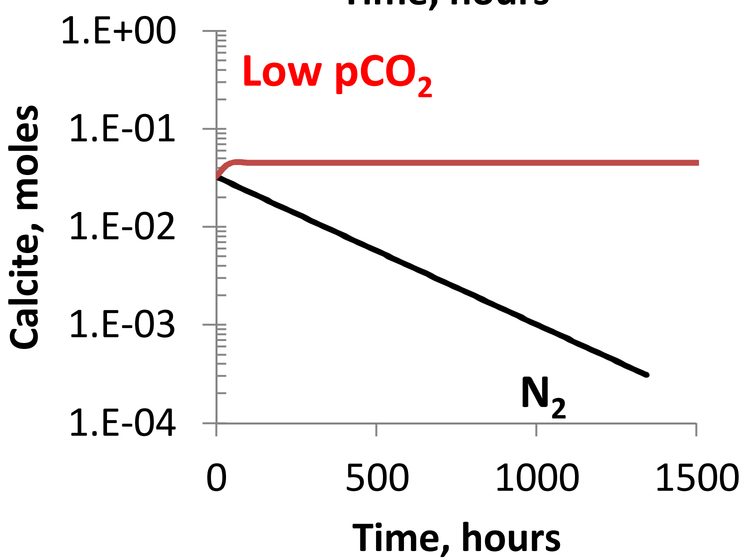

- Calcite dissolution/precipitation and gypsum precipitation are the predominant mineralogical changes on the time scale of the experiment.
- Model predicts: minor amount of brucite in N_2-pressurized reactor, and magnesite and gibbsite– in CO_2-pressurized reactor.

XRD, XRF: Mancos

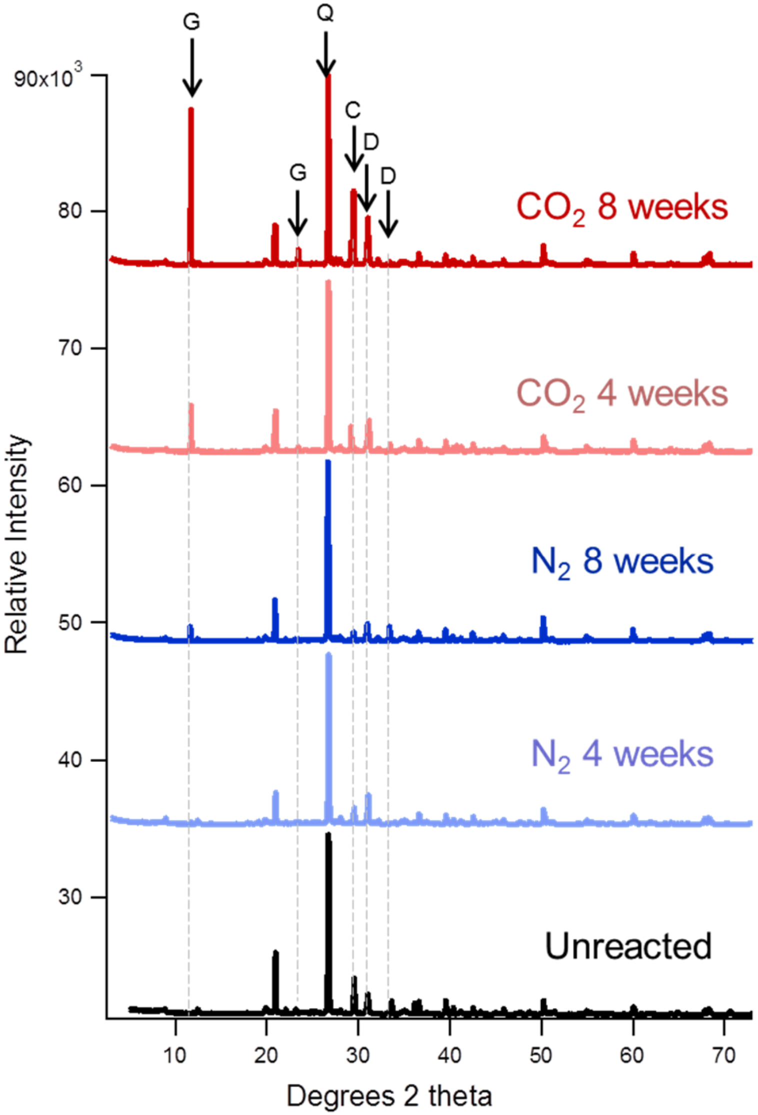

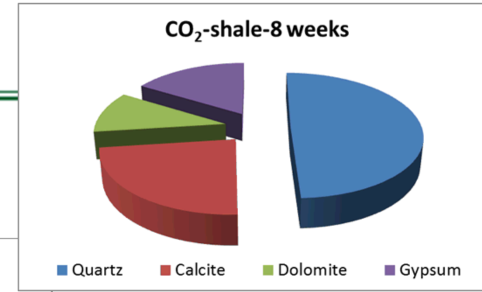

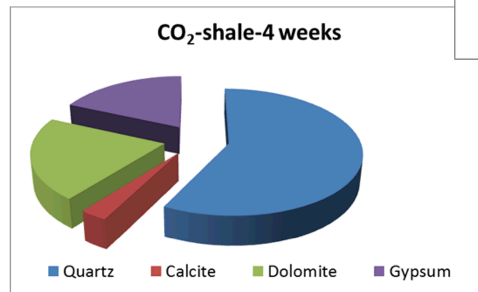

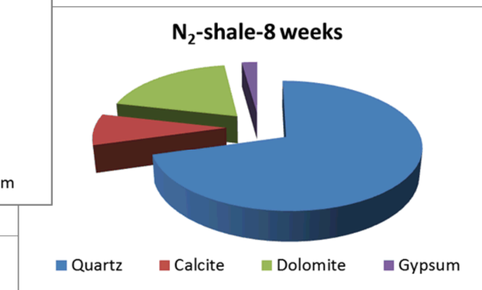

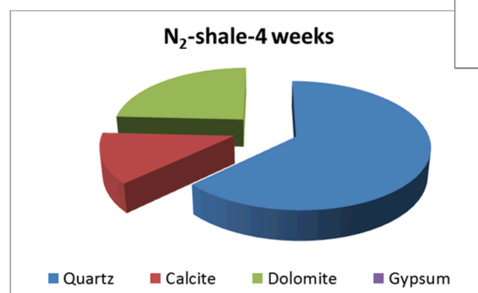

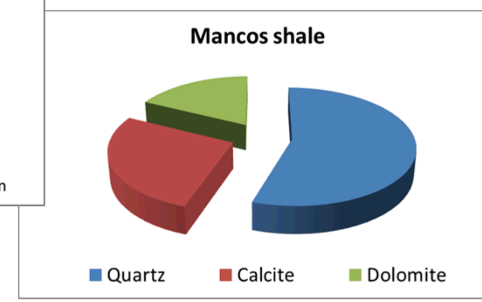

XRF

Reactor	Mg	Al	Si	S	K	Ca	Fe
CO_2	1.78	7.66	53.16	11.32	4.23	12.55	7.61
N_2	2.62	7.06	54.7	4.56	2.61	14.41	11.61

Mancos shale: Conclusions

Laboratory study

$$\underset{\text{calcite}}{CaCO_{3(s)}} + 2H^+ \rightarrow Ca^{2+} + H_2CO_3$$

$$\underset{\text{dolomite}}{CaMg(CO_3)_{2(s)}} + 4H^+ \rightarrow Ca^{2+} + Mg^{2+} + 2H_2CO_3$$

$$Mg^{2+} + H_2CO_3 \rightarrow \underset{\text{magnesite}}{MgCO_{3\,(s)}} + 2H^+$$

$$Ca^{2+} + H_2CO_3 \rightarrow \underset{\text{calcite}}{CaCO_{3\,(s)}} + 2H^+$$

$$Ca^{2+} + SO_4^{2-} \rightarrow \underset{\text{gypsum}}{CaSO_{4\,(s)}} + 2H^+$$

$$\underset{\text{muscovite}}{KAl_3Si_3O_{10}(OH)_{2(s)}} + 4H_2O \rightarrow \underset{\text{gibbsite}}{3Al(OH)_{3(s)}} + 3SiO_2 + K^+ + OH^-$$

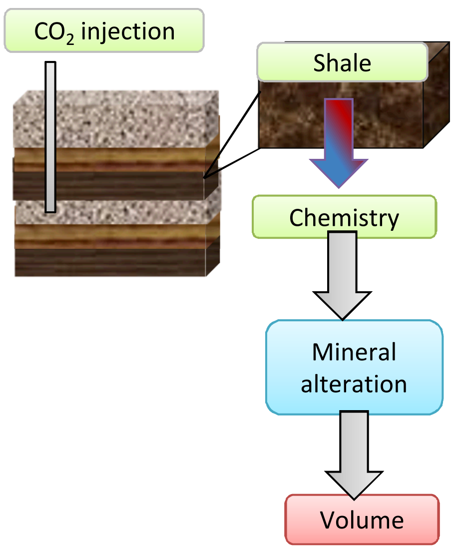

Mineral	Calcite	Albite	Dolomite	Muscovite
ρ, g cm^{-3}	2.71	2.62	2.84	2.82
Hardness	3	7	3.5 - 4	2 - 2.5
Mineral	**Calcite**	**Gypsum**	**Magnesite**	**Gibbsite**
ρ, g cm^{-3}	2.71	2.3	3	2.42
Hardness	3	2	4	3

Alteration by CO_2-brine mixture maybe causing net decrease in density and hardness.

Fractures in CO_2 caprocks: Crystal Geyser analog site

Field study

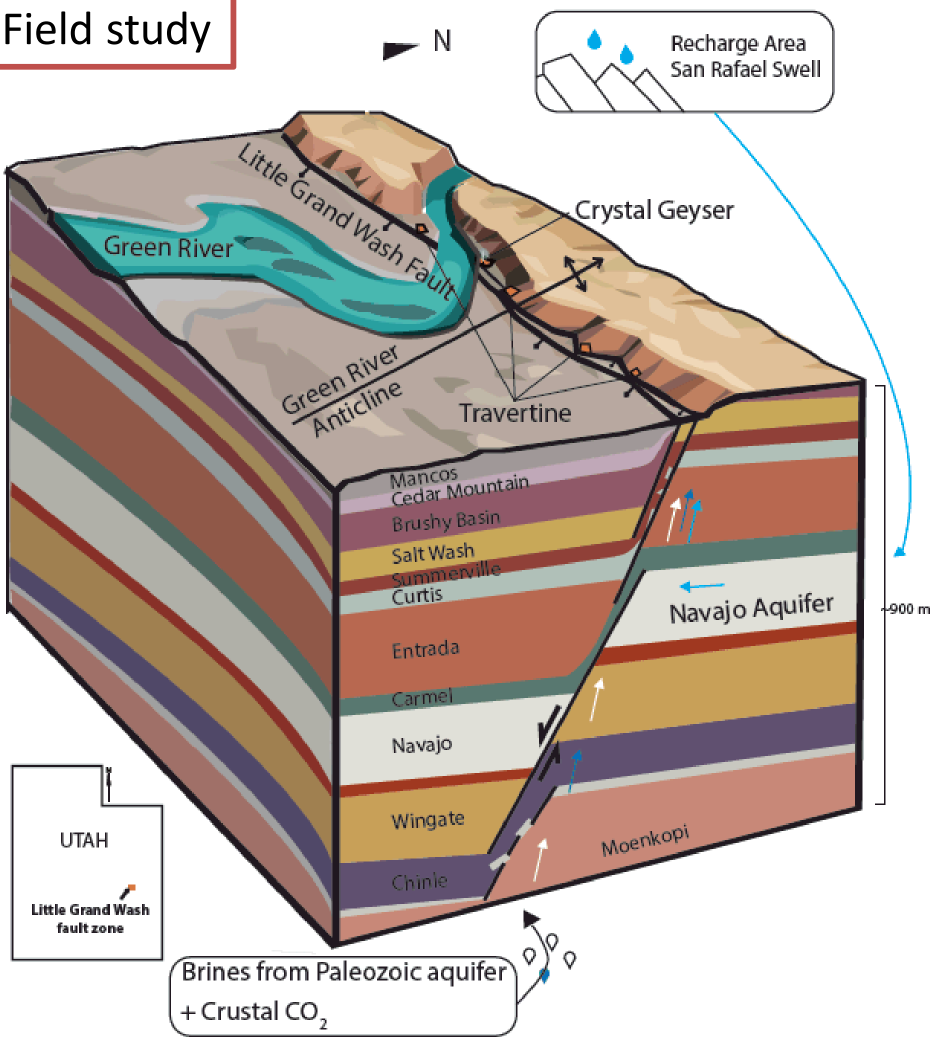

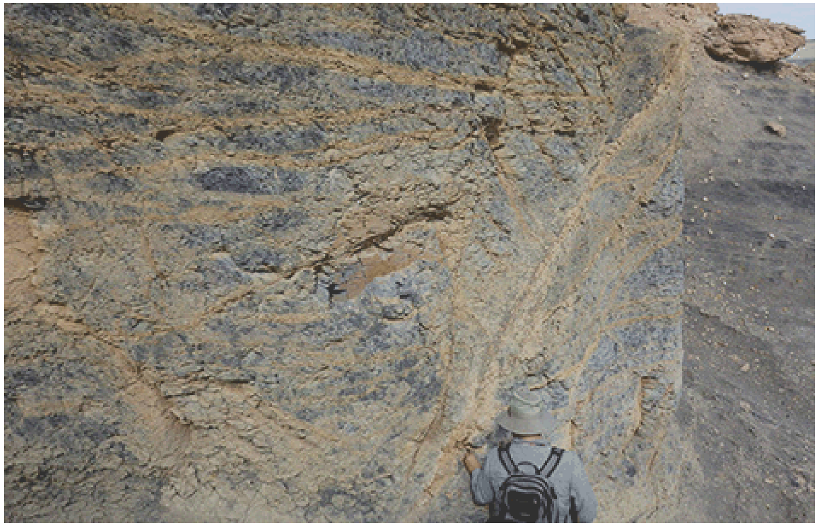

Active on 10^2 - 10^5 year time scales

Compositional changes of mudrock

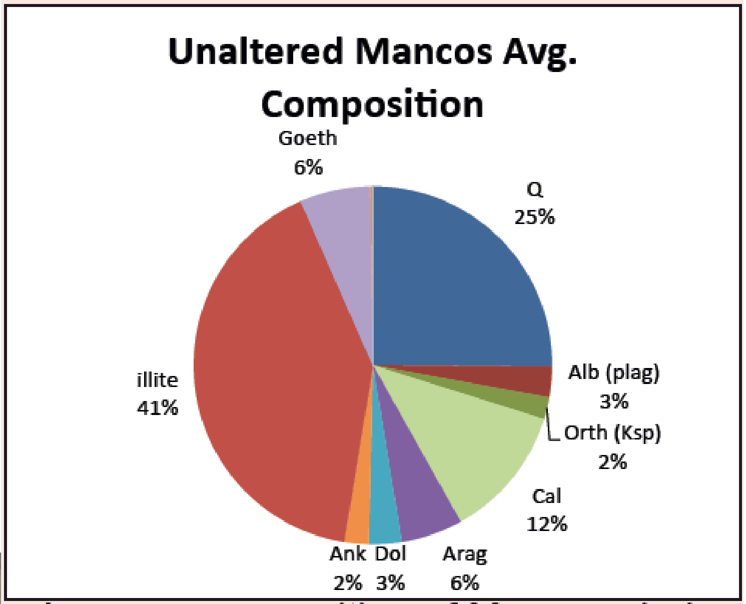

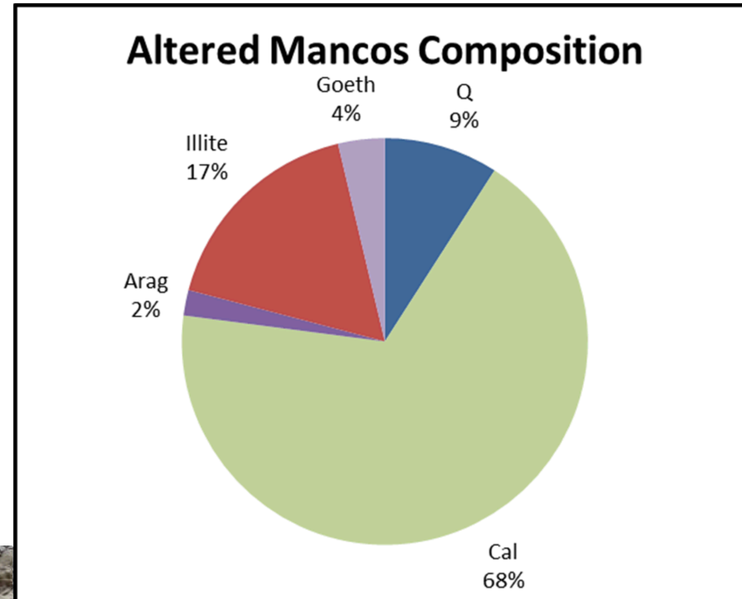

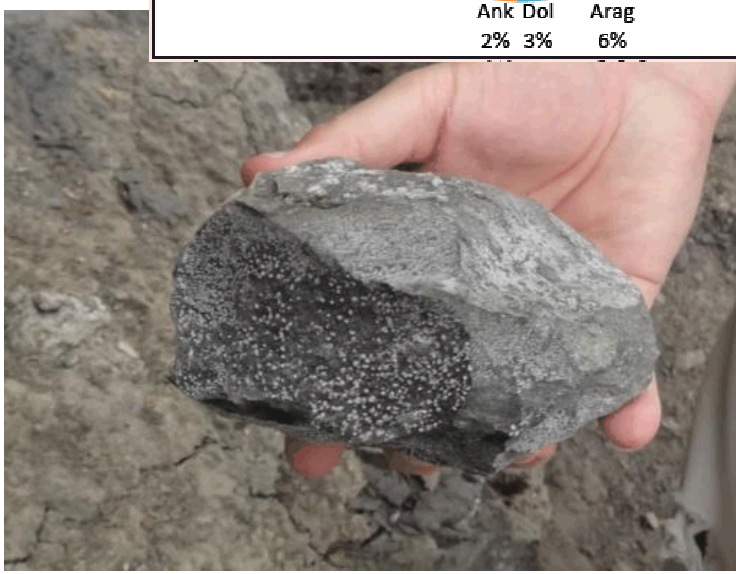

Field fracture characterization in natural CO_2 systems

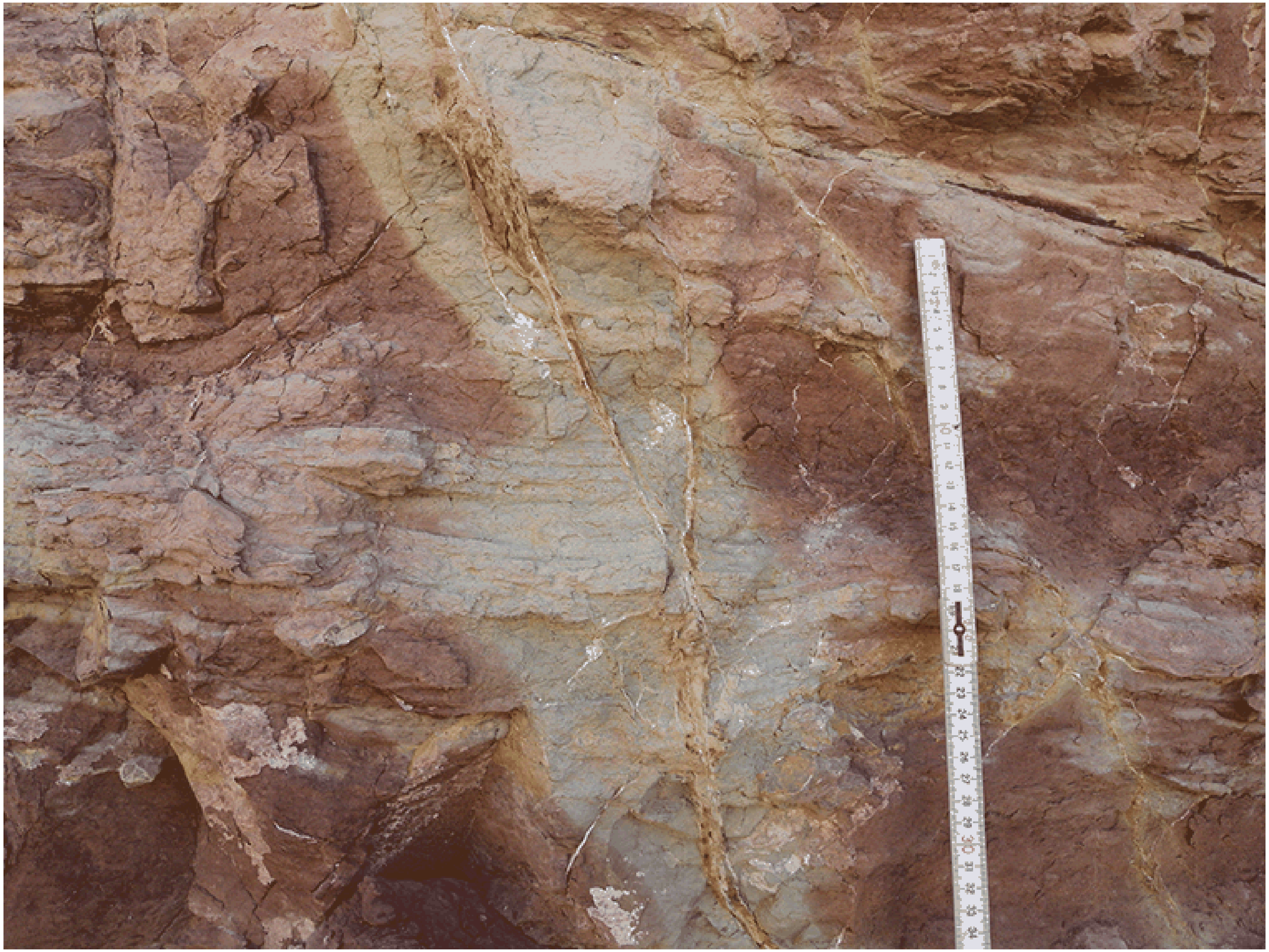

Double torsion testing: Fracture toughness, subcritical crack index n (SCI)

Field study

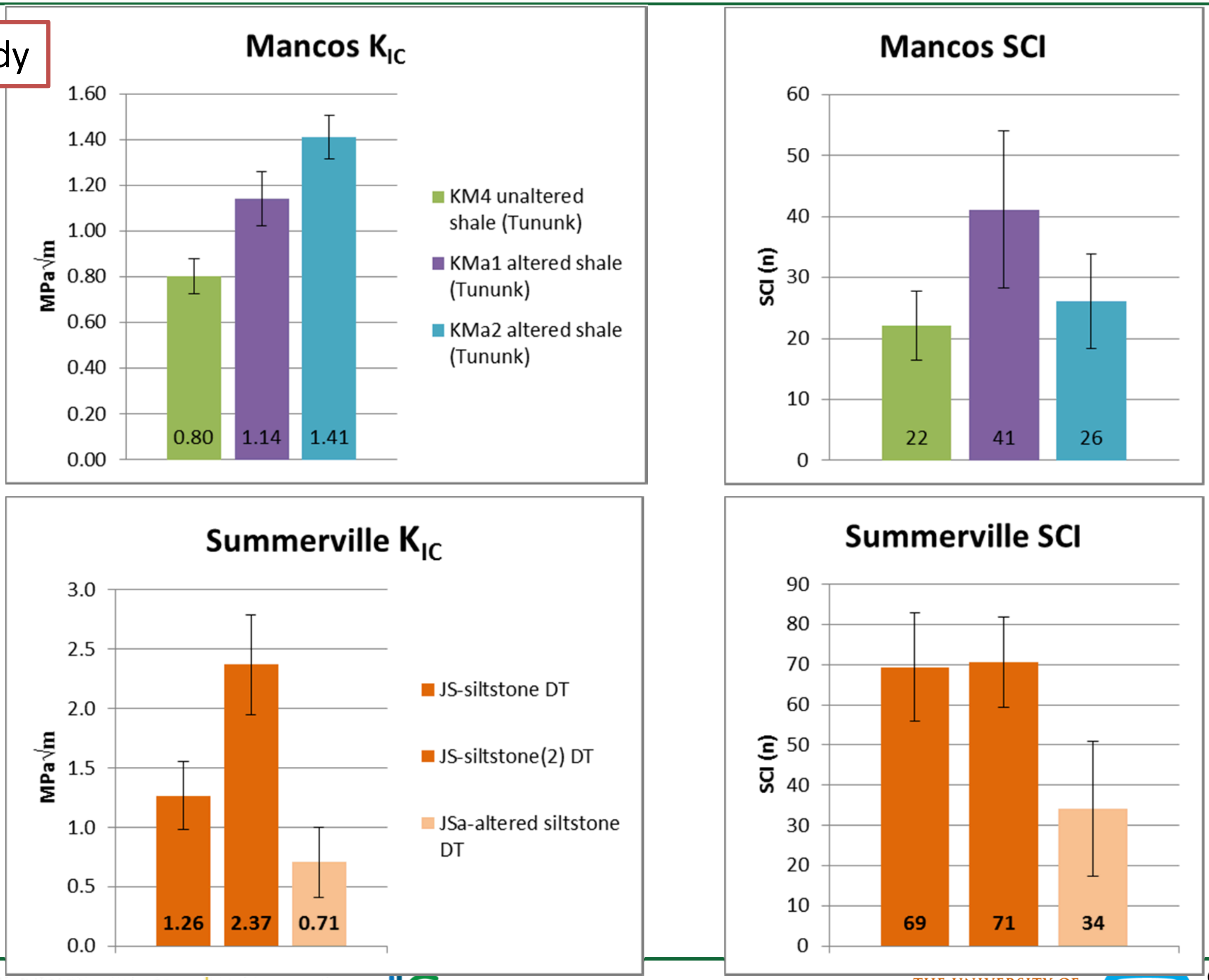

Aqueous chemistry: Woodford

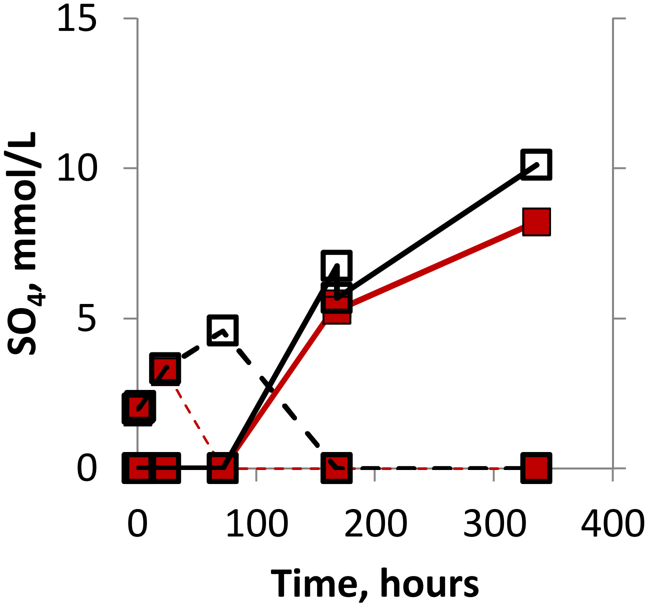

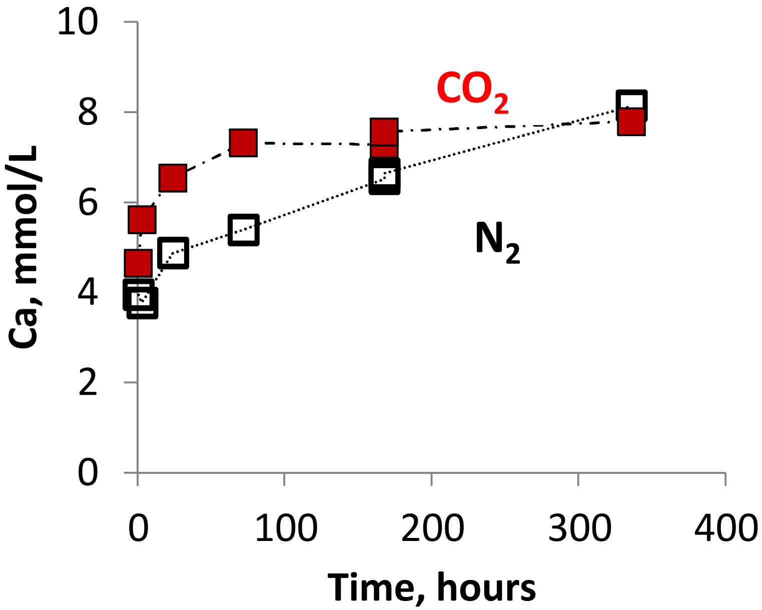

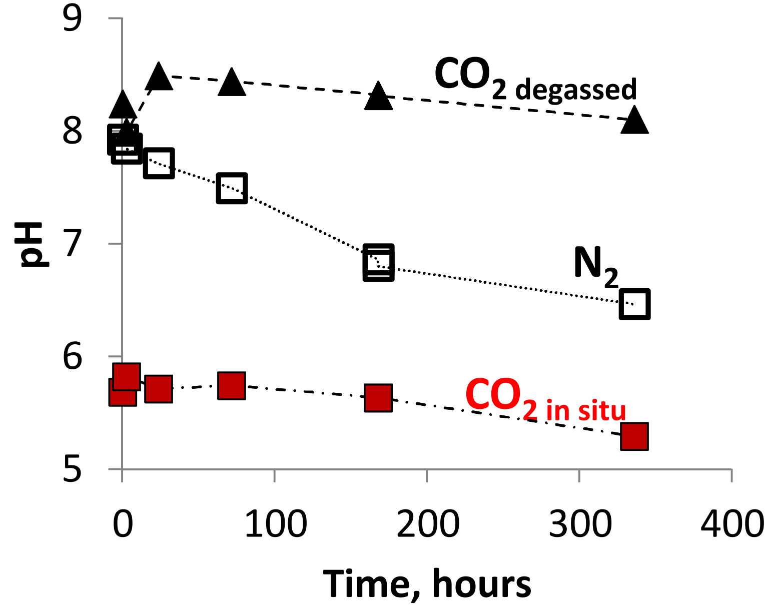

- TDS is ~ constant
- Ca, Mg, and Si are more soluble in CO_2 vs. N_2 reactor.
- Al and Fe - very low, umol/L level (Al), 0.1 umol/L (Fe).
- No Na-K cation exchange
- SO_4 consumption, PO_4 mobilization.

XRD: Woodford

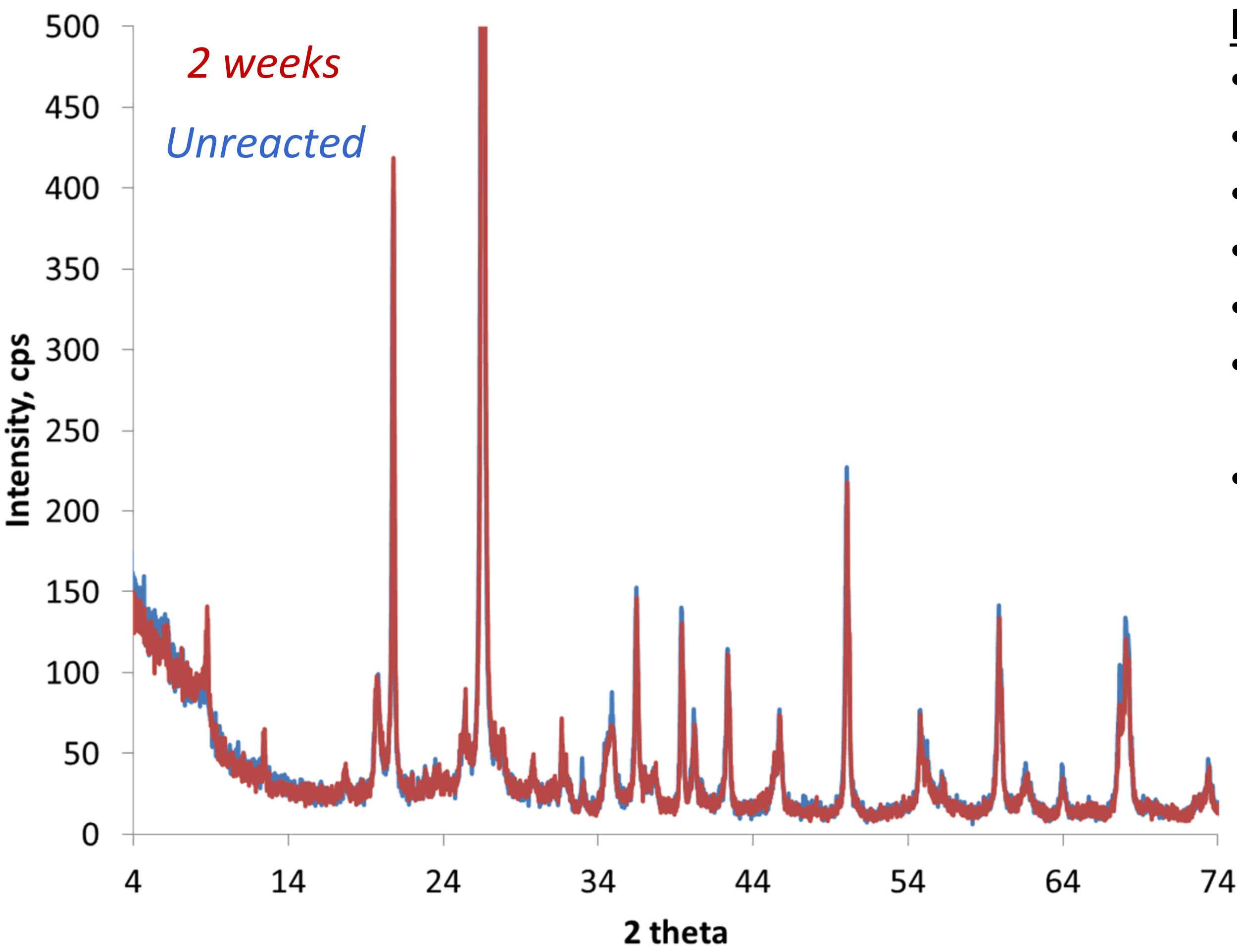

Initial composition:

- Quartz
- Illite, mica
- Chlorite
- Anhydrite
- Calcite (small amount)
- Plagioclase

- No dolomite

What's dissolving:

- Quartz
- Calcite

After 2 weeks

Future work

Experiments

Geochemistry	Geomechanics
Alteration of Woodford and Eau Claire shales in brine-CO_2 systems at high and low pressure of CO_2	Micromechanical experiments: nano-pillar indentation to measure mechanical changes due to alteration by CO_2.
Effect of gas impurities (O_2, and potentially NOx, and SOx) on the minerals alteration in CO_2-brine systems.	Micromechanical experiments: indentation and scratch test to measure mechanical alteration by CO_2.

Modeling

Geochemistry	Geomechanics
Geochemical modeling to interpret observed geochemical changes and construct predictive models for the carbon storage time scales (1000 years and longer).	Integrating computation with micromechanical (indention and scratch) experiments, using the DEM and FEM approaches with coupling of geochemistry and mechanics.

Micro-mechanical characterization: scratch tests

- Micromechanical experiments (scratch test) to measure mechanical alteration by CO_2 and identify characteristic time-scales and length-scales involved in the geochemical reactive transport processes.

Apparatus for scratch test

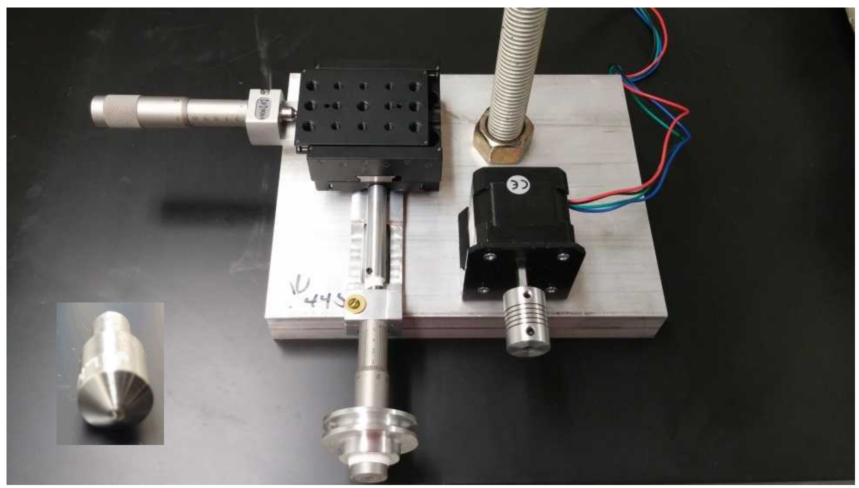

Micromechanical Properties

Micron scale laboratory experiments on unaltered and chemically altered shales to assess changes in mechanical properties like hardness, Young's Modulus, and unconfined compressive strength due to chemical reactions likely to occur with $scCO_2$ in GCS. Results can be applied to assess long-term caprock stability.

Nano-pillar indentation	Micropillar compression
An AFM based tool, this utilizes a rigid punch to indent a machined smooth surface of a sample to calculate hardness and Young's modulus. Automation allows for high density surface coverage to map changes in properties. Different indentation depths test different volumes of materials.	Analogous to standard geomechanics tests, pillars are machined into sample surface using FIB, and deformed with a rigid punch in SEM to measure UCS and Young's modulus. The small size of the pillars allows the testing of individual mineral constituents to determine mechanical properties.

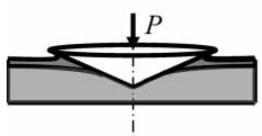

Tang & Ngan, 2007

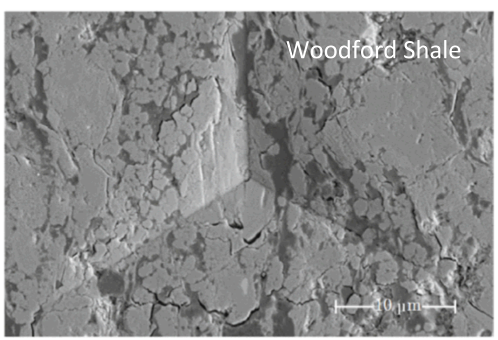

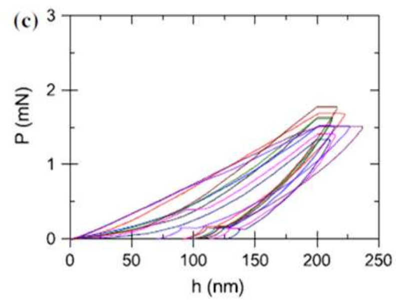

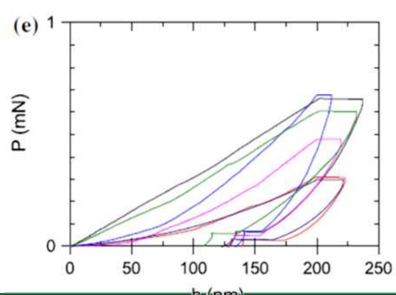

Bennett et al., 2015

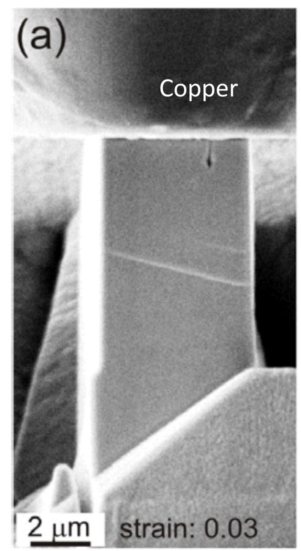

Kiener et al., 2011

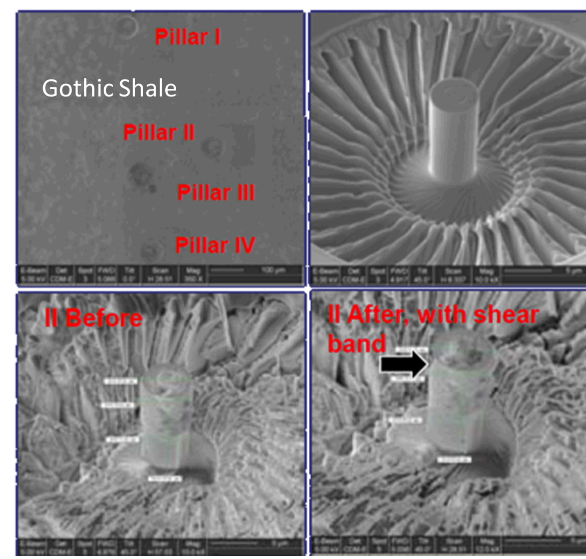

Dewers et al., 2010

Computational model

- **Discrete Element Method (DEM) Particle Fracture Model**
  - Poly-ellipsoidal DEM Particle Fracture Model (bonding for chemistry effect)

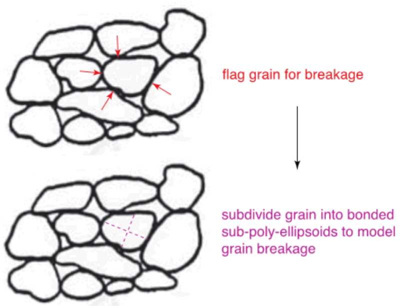

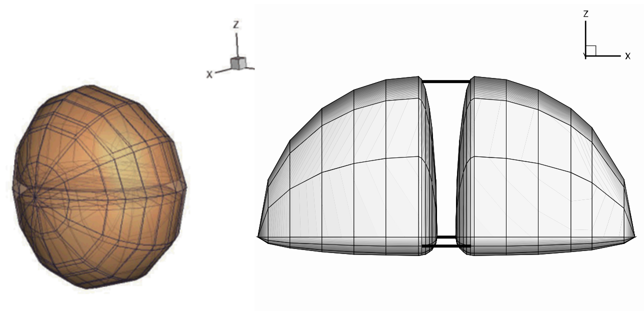

Zhang et al., 2015, LLNL

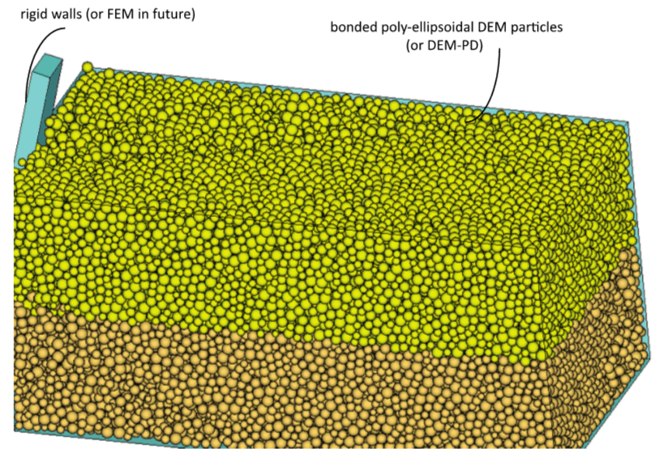

Rizo, 2013, University of Pittsburgh, PhD Thesis

- **Finite Element Method (FEM)**
  - XFEM-Presto (Sierra Mechanics)
  - Kayenta as constitutive model

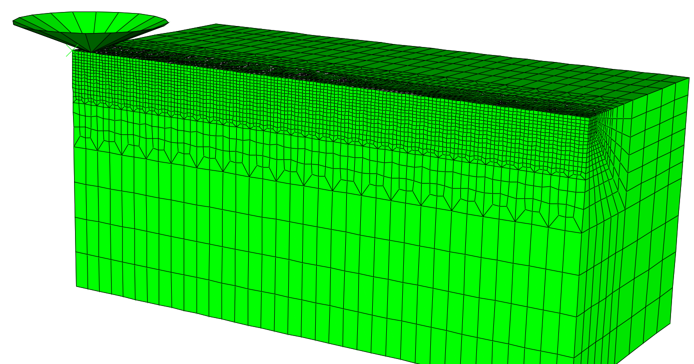

Wredenberg and Larsson , 2007

CFSES Research Challenges and Efforts

Sustaining Injectivity

Storage Efficiency

Long-term security of CO_2 storage

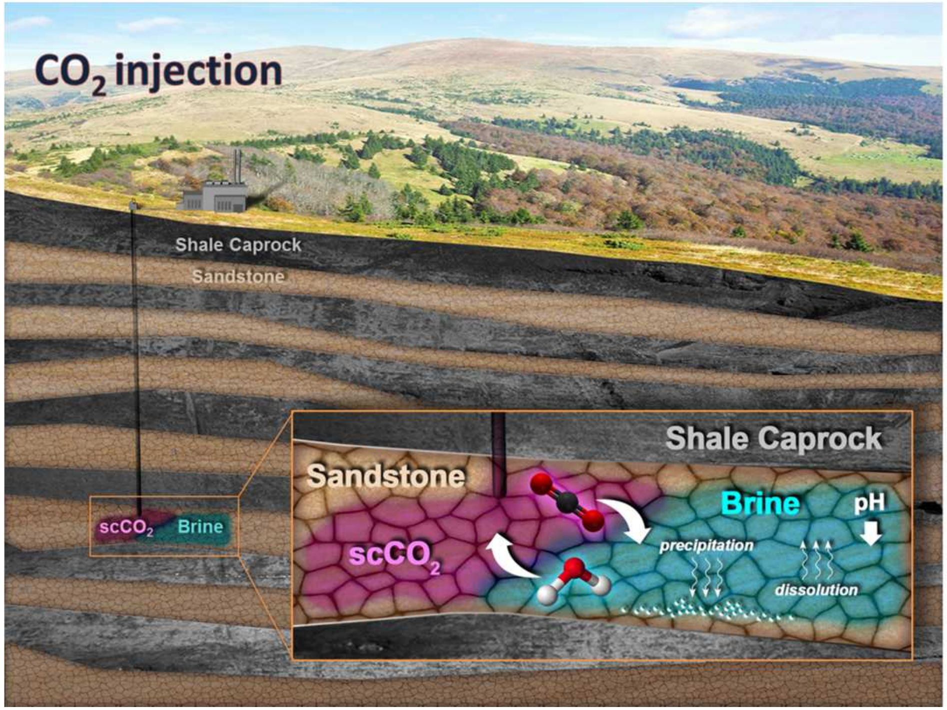

Controlling Emergence

Caprock alteration experiments will help understanding the coupled geochemical-geomechanical processes and developing strategies for controlling CO_2 leakage pathway development.

Alteration by brine-CO_2 influences mechanical integrity of rock types in different ways depending on mineral make up and brine chemistry, and extent of alteration.

Acknowledgements

People Mark Rodriguez and James Griego, SNL – XRD and XRF analysis
Mona Aragon, SNL – CO_2 injection graphics

Funding Center for Frontiers of Subsurface Energy Security, an Energy Frontier Research Center funded by the U.S. Department of Energy, Office of Science, Office of Basic Energy Sciences under Award Number DE-SC0001114.

Sandia National Laboratories is a multi-program laboratory managed and operated by Sandia Corporation, a wholly owned subsidiary of Lockheed Martin Corporation, for the U.S. Department of Energy's National Nuclear Security Administration under contract DE-AC04-94AL85000.

U.S. DEPARTMENT OF ENERGY | Office of Science
CFSES Center for Frontiers of Subsurface Energy Security
THE UNIVERSITY OF TEXAS AT AUSTIN
Sandia National Laboratories

Extra slides

Subcritical fracture growth

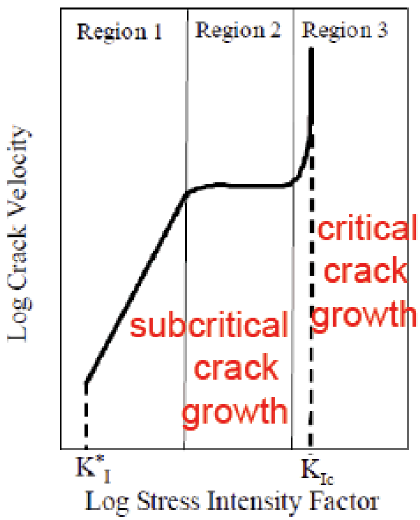

K^*_I = stress corrosion limit
K_{IC} = fracture toughness

After Atkinson, 1984

$$V = A\left(\frac{K_I}{K_{IC}}\right)^n$$

V: fracture propagation velocity
K_I: mode-I stress intensity factor,
K_{IC}: mode-I critical stress intensity factor (or fracture toughness)
A: a pre-exponential constant (Atkinson, 1984; Swanson 1984)
n: velocity exponent (SCI)

Results of subcritical crack growth affecting fracture network geometry

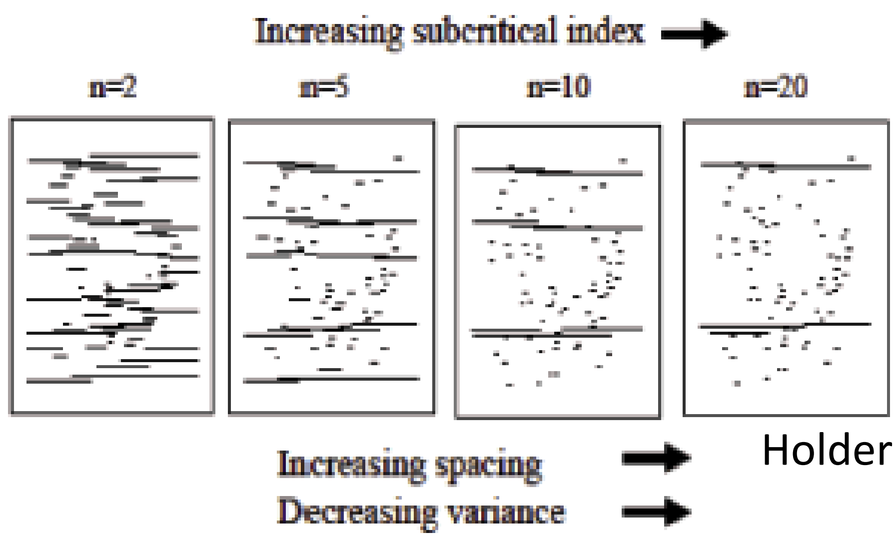

Holder et. al, 2001

Double torsion fracture mechanics testing

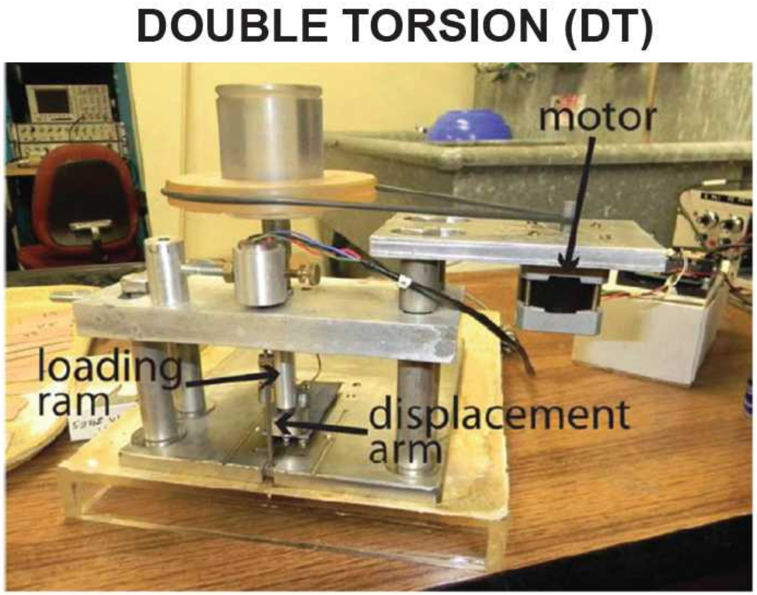

Hot plate & tray for temperature and fluid control

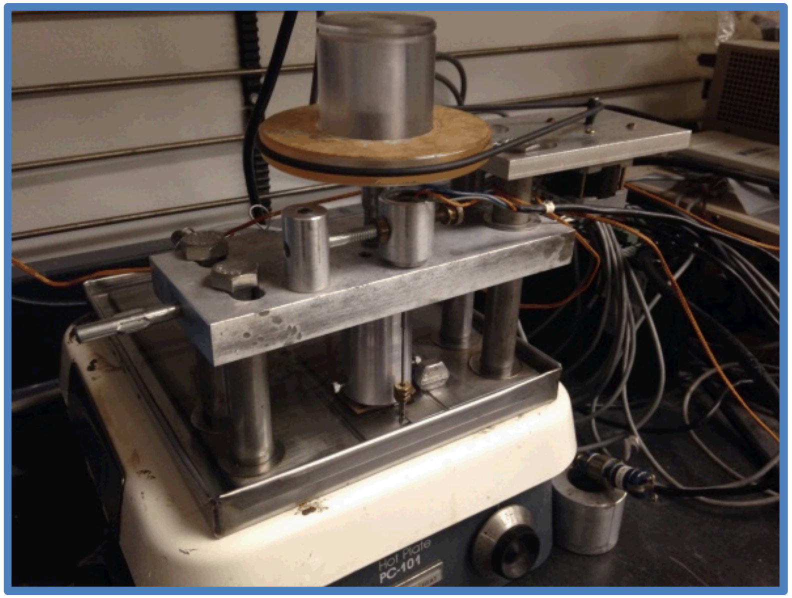

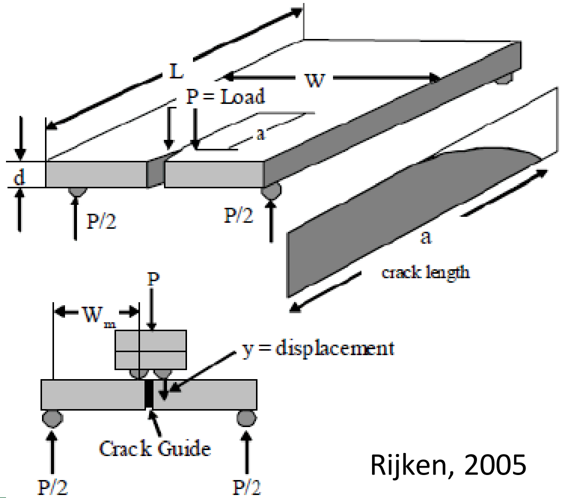

Rijken, 2005

Sample geometry

Aqueous chemistry: Mancos

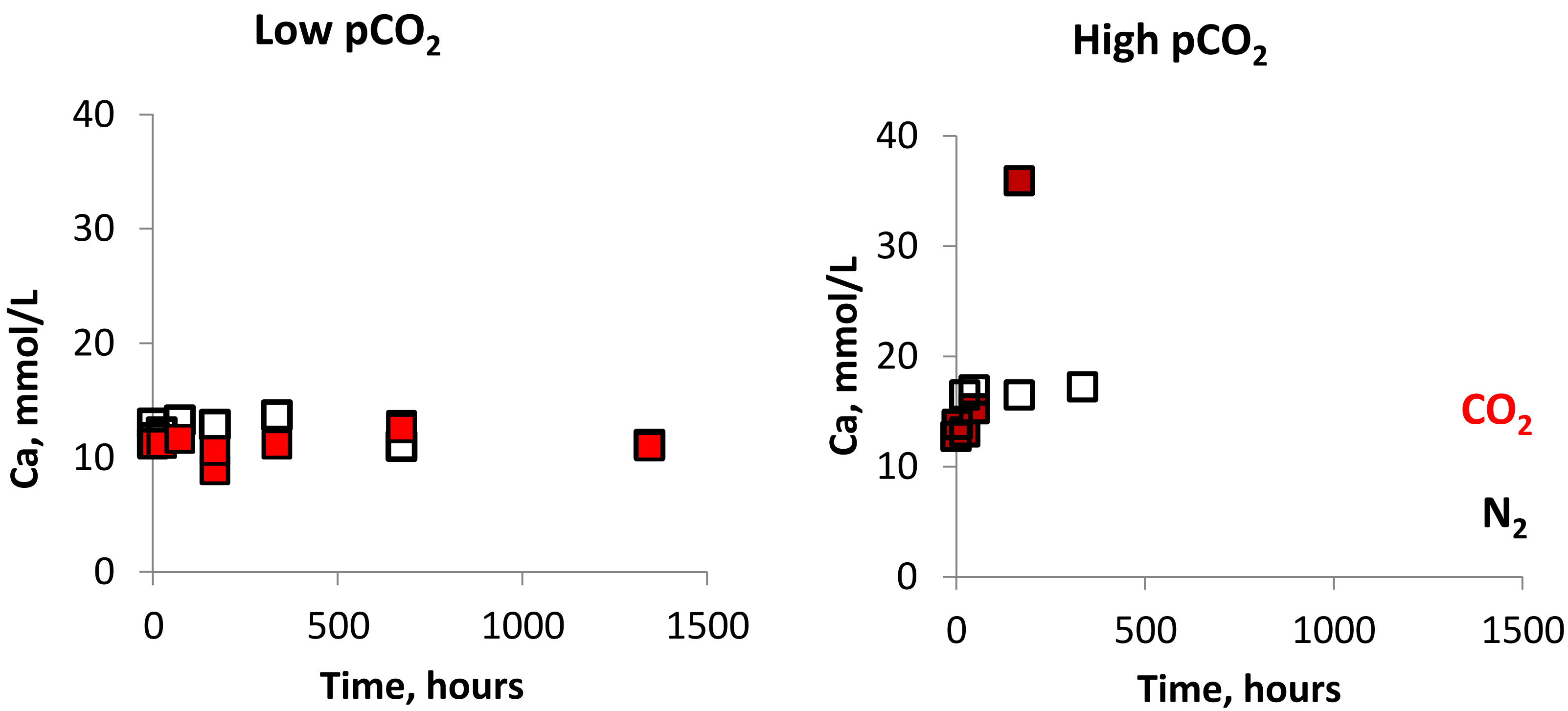

- Ca is more soluble in high p-CO_2 -pressurized reactor

Aqueous chemistry: Mancos

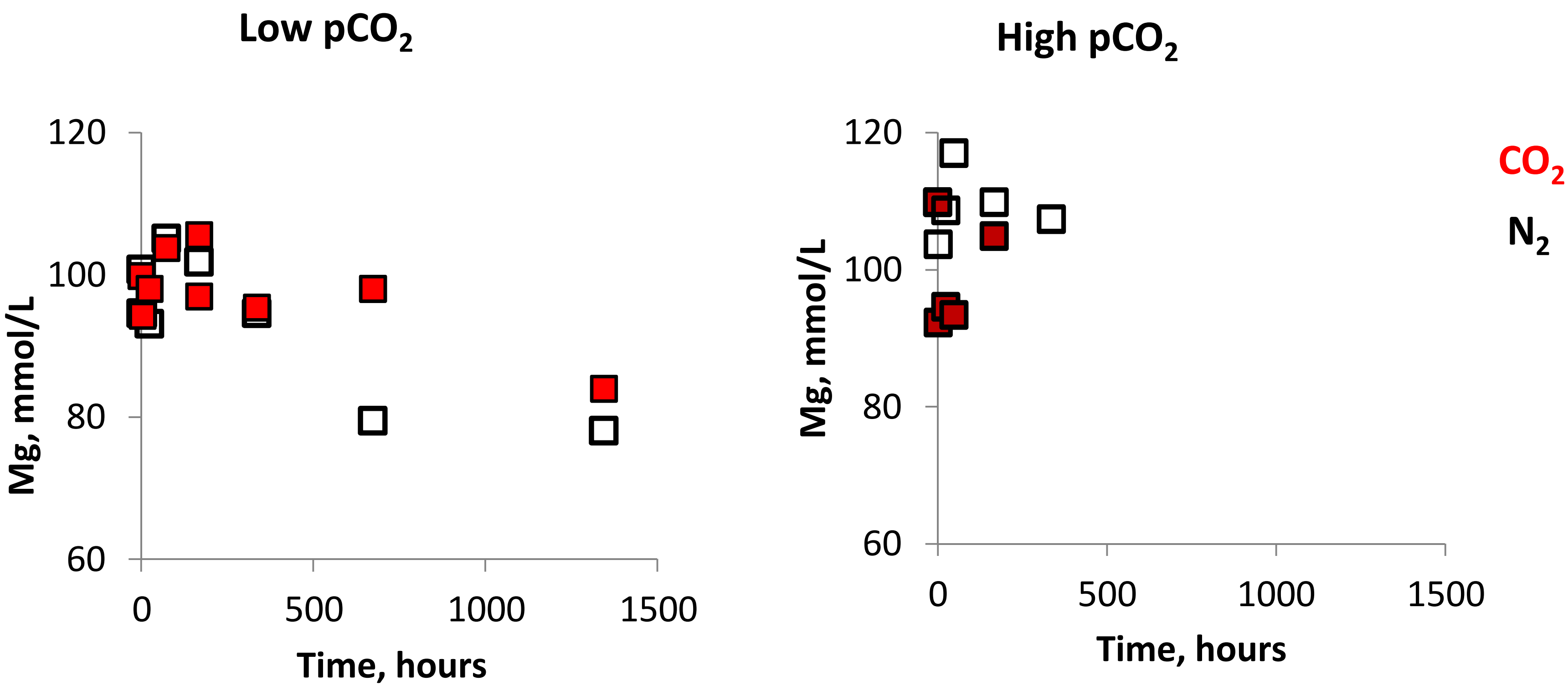

- Ca, Mg, Si, Sr, and Fe are more soluble in CO_2 vs. N_2 and atm reactors; Al – not detected.

Aqueous chemistry: Mancos

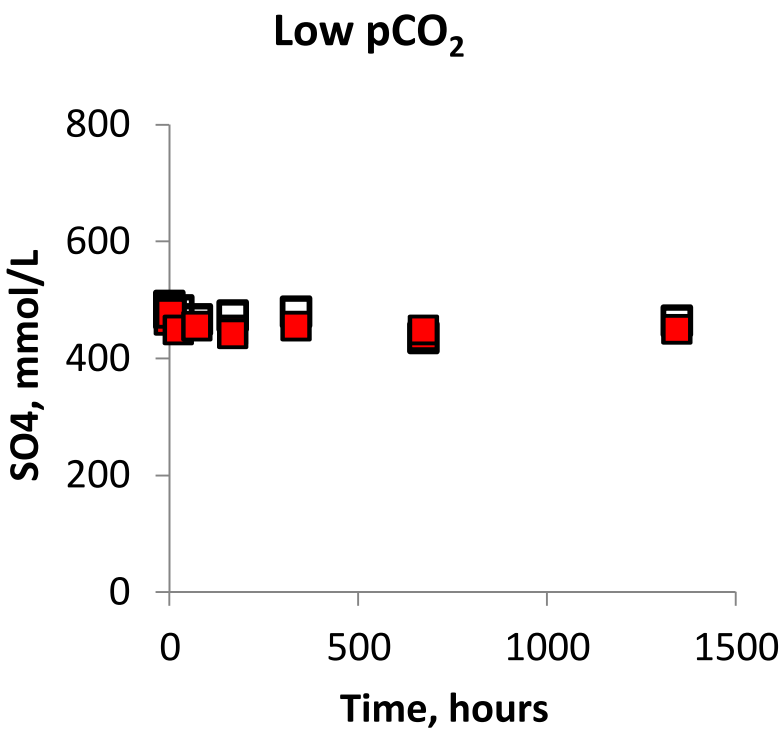

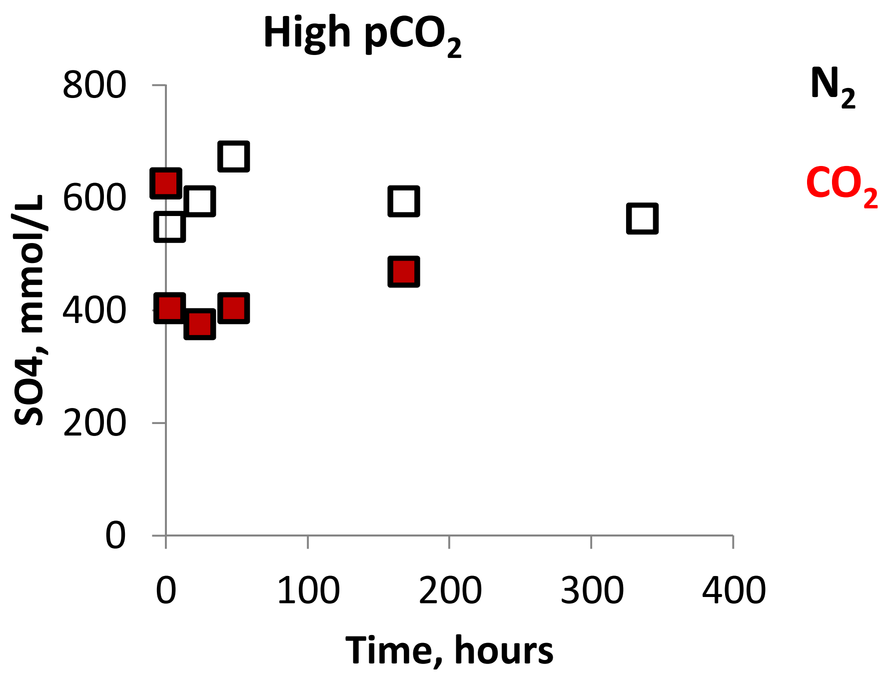

- Ca, Mg, Si, Sr, and Fe are more soluble in CO_2 vs. N_2 -pressurized reactor; Al – not detected.
- Positive Na-K correlation indicates no cation exchange.

Aqueous chemistry: Mancos

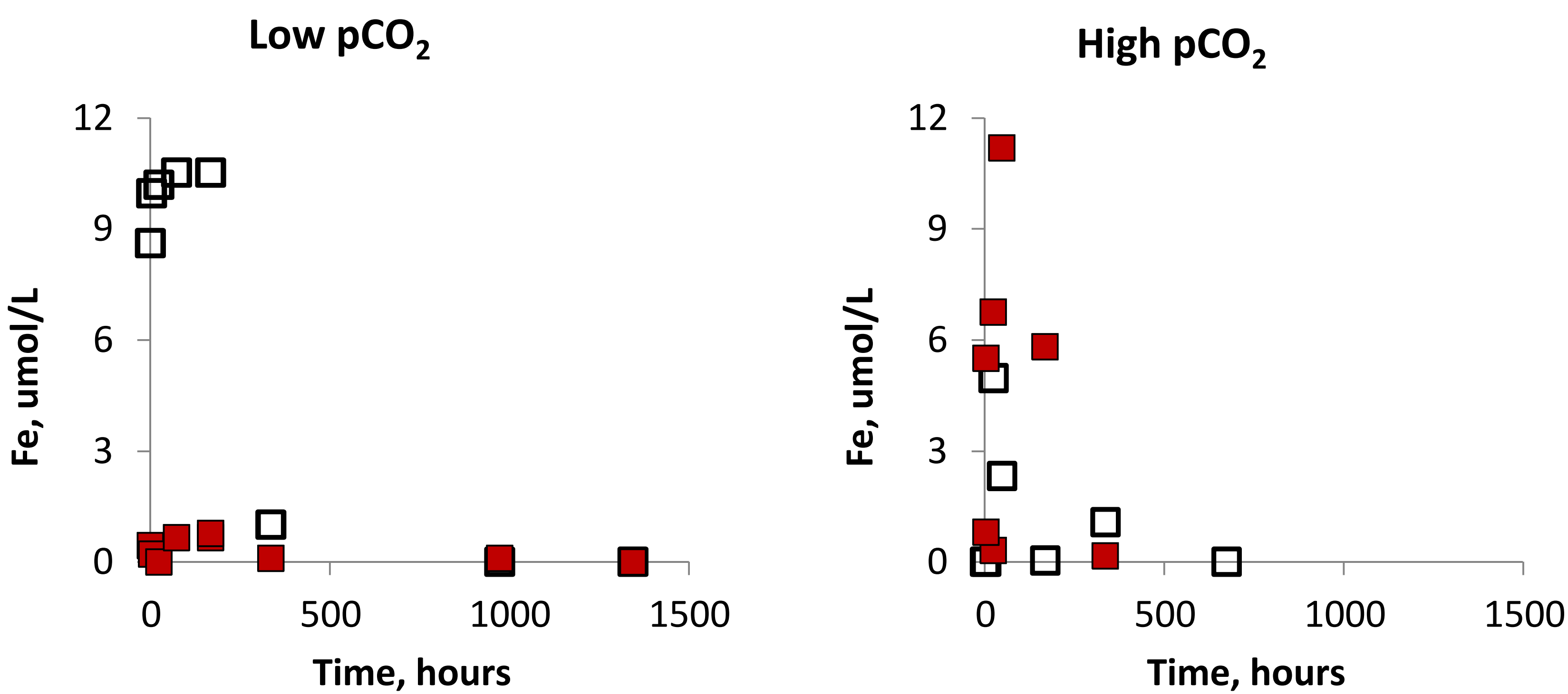

- Fe is more soluble in high p-CO_2 -pressurized reactor

Aqueous chemistry: Mancos

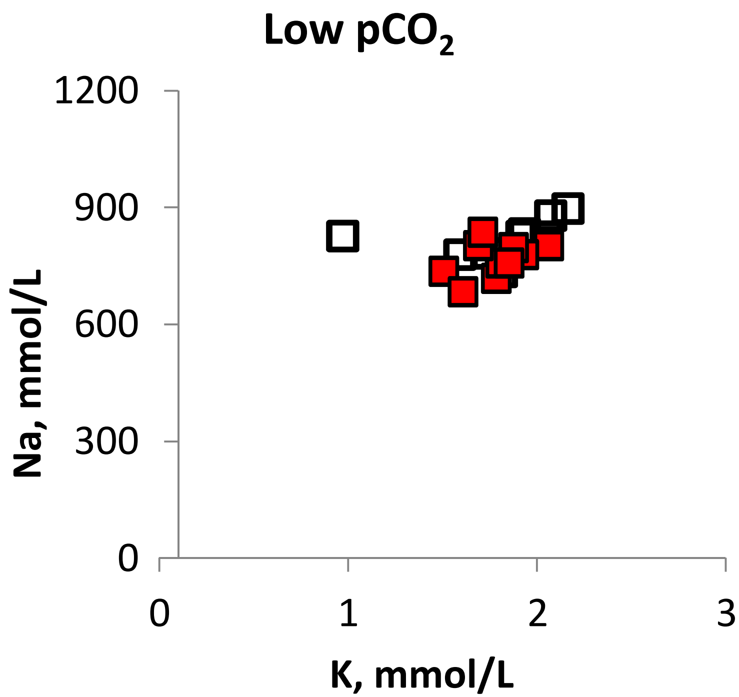

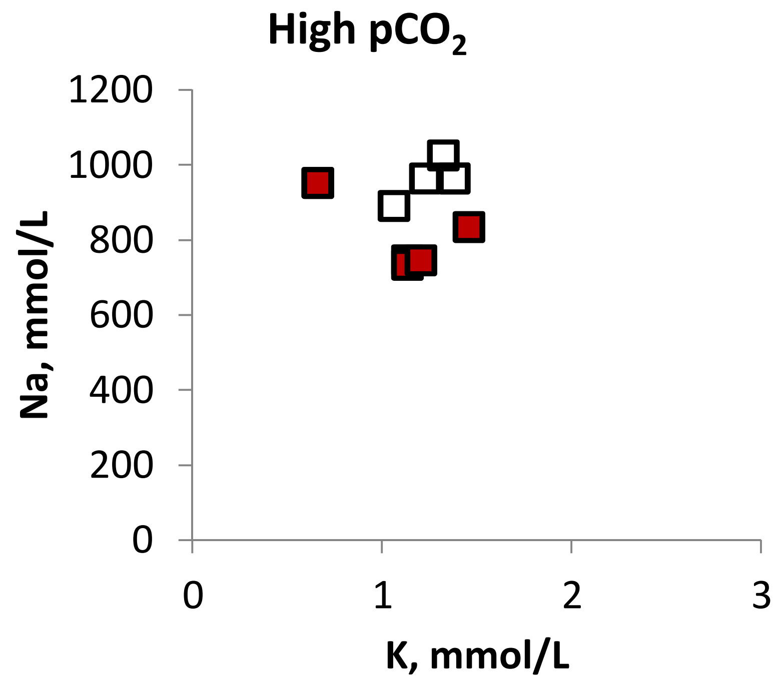

- Positive Na-K correlation indicates no cation exchange.

XRF: Mancos

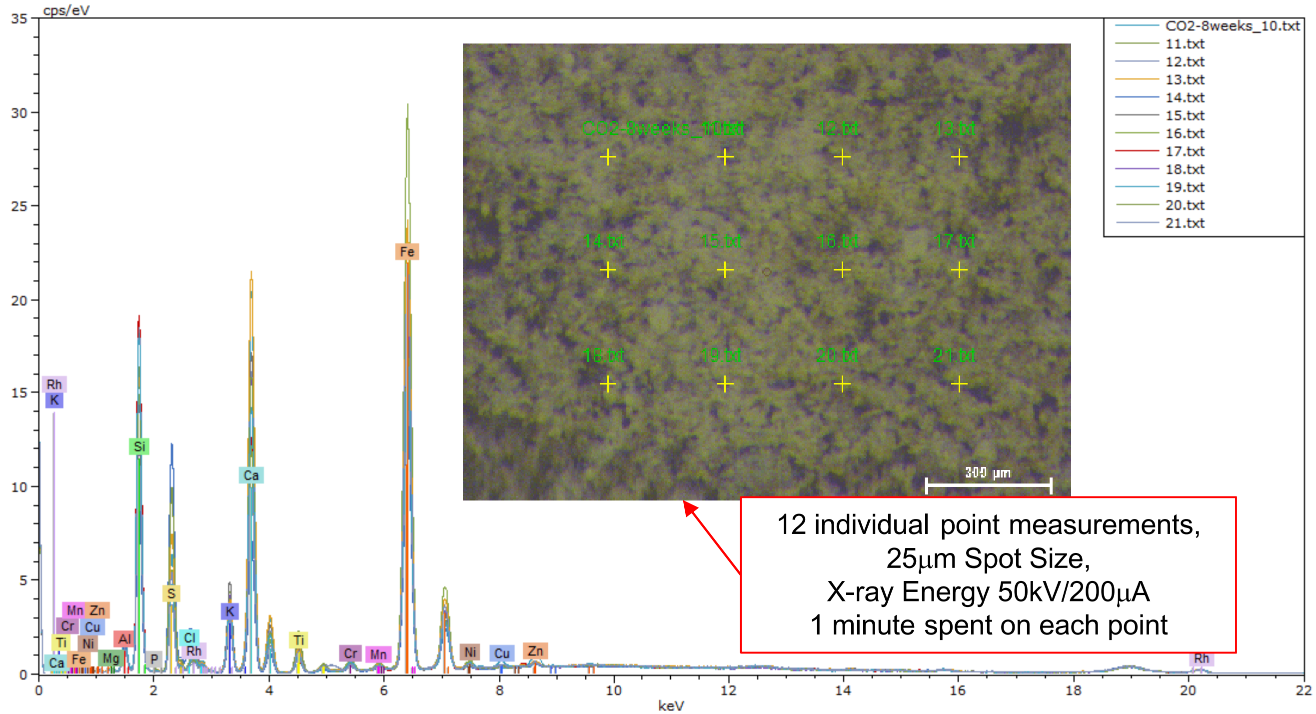

Reactor	Mg	Al	Si	S	K	Ca	Fe
CO_2	1.78	7.66	53.16	11.32	4.23	12.55	7.61
N_2	2.62	7.06	54.7	4.56	2.61	14.41	11.61

Geochemical Modeling: Mancos

- Path of reaction modeling using Geochemists Work Bench (Bethke, 1998).

Initial brine		
pH	7.44	
Cl^-	1589	mg/L
NO_3^-	4.1	mg/L
SO_4^{2-}	47251	mg/L
K^+	20.5	mg/L
Ca^{2+}	484	mg/L
Na^+	19000	mg/L
Mg^{2+}	2700	mg/L
Fe^{2+}	2	mg/L

Mineral	wt.%	k, mol cm^{-2} sec^{-1}
Quartz	80.5	1×10^{-17}
Albite	8.3	1×10^{-16}
Dolomite	7.6	1×10^{-12}
Calcite	4.9	1×10^{-8}
Muscovite	2	1×10^{-14}
Kaolinite	1	1×10^{-14}
Pyrite	1	2.5×10^{-15}
Hematite	1	2.5×10^{-14}

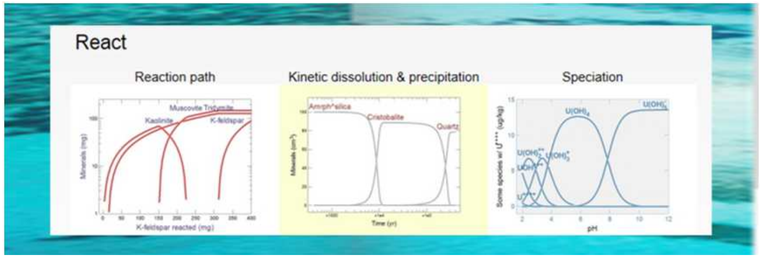

Image source: http://www.gwb.com/